Paleobiology, 35(4), 2009, pp. 565–586

Taphonomic bias and time-averaging in tropical molluscan death assemblages: differential shell half-lives in Great Barrier Reef sediment

Matthew A. Kosnik, Quan Hua, Darrell S. Kaufman, and Raphael A. Wüst

Abstract.—Radiocarbon-calibrated amino acid racemization ages of 428 individually dated shells representing four molluscan taxa are used to quantify time-averaging and shell half-lives with increasing burial depth in the shallow-water carbonate lagoon of Rib Reef, central Great Barrier Reef, Australia. The top 20 cm of sediment contains a distinct, essentially modern assemblage. Shells recovered at depths from 25 to 125 cm are age-homogeneous and significantly older than the surface layer. Taxon age distributions within sedimentary layers indicate that the top 125 cm of lagoonal sediment is thoroughly mixed on a sub-century scale. The age distributions and shell half-lives of four taxa (*Ethalia*, *Natica*, *Tellina*, and *Turbo*) are found to be largely distinct. Shell half-lives do not coincide with any single morphological characteristic thought to infer greater durability, but they are strongly related to a combined durability score based on shell density, thickness, and shape. These results illustrate the importance of bioturbation in tropical sedimentary environments, indicate that age estimates in this depositional setting are sensitive to taxon choice, and quantify a taxon-dependent bias in shell longevity and death assemblage formation.

Matthew A. Kosnik. School of Marine and Tropical Biology, James Cook University, Townsville, Queensland 4811, Australia*

Quan Hua. Australian Nuclear Science and Technology Organisation, PMB 1, Menai, New South Wales 2234, Australia. E-mail: qhx@ansto.gov.au

Darrell S. Kaufman. Department of Geology, Northern Arizona University, Flagstaff, Arizona 86011-4099, E-mail: Darrell.Kaufman@nau.edu

Raphael A. Wüst. School of Earth and Environmental Sciences, James Cook University, Townsville, Queensland 4811, Australia. E-mail: Raphael.Wust@jcu.edu.au

*Present address: *Department of Paleobiology, National Museum of Natural History, Smithsonian Institution, Post Office Box 37012, NHB MRC 121, Washington, D.C. 20013-7012. E-mail: mkosnik@alumni.uchicago.edu*

Accepted: 2 February 2009

Introduction

Determining the geochronological framework and potential age biases of sedimentary sequences is of paramount importance for studying modern and past sedimentary systems. Sediments contain or, in the case of carbonate deposits, are composed of various shells and carbonate fragments of multiple origins and ages. Although the range of ages in a single sediment sample (i.e., time-averaging) is one of the most basic sedimentological parameters, it is one of the least quantified. Time-averaging determines the length of time represented by a stratigraphic unit and limits the temporal resolution of a given record (Flessa et al. 1993; Kowalewski 1996). The geochronological framework of most sedimentary sequences is determined by relatively few biological specimens. The underlying *true* age of interest is, however, the *unknown* age distribution of all biological constituents within the sedimentary layer. Quantifying the age distribution is time and resource intensive, so although time-averaging is of utmost importance for processes underlying nearly all paleontological and sedimentological investigations, few studies have included a sufficient number of specimens to quantify the age-frequency distribution.

Time-averaging is fundamentally determined by three largely independent parameters: (1) the rate of sediment accumulation; (2) the characteristics of sediment mixing; and (3) the durability of the sedimentary grains being averaged. The sedimentation rate determines the minimum possible degree of time-averaging, and generally higher rates of sedimentation lead to less time-averaging (Meldahl et al. 1997). The rate and depth of mixing

 0094-8373/09/3504–0006/$1.00

determine the maximum possible degree of time-averaging, with deeper and faster sediment mixing leading to more time-averaging (Olszewski 2004). Some bioturbators (e.g., callianassid shrimp) also effectively sort sedimentary grains by size, shape, and/or other characteristics (Tudhope and Scoffin 1984). Sediment grain durability determines the length of time that a sedimentary particle remains intact and recognizable. Fragile sedimentary particles are more likely to be destroyed (e.g., fragmented, eroded, or dissolved) during mixing, leading to less time-averaging, whereas durable particles can be thoroughly mixed without breaking, leading to more time-averaging (Cummins et al. 1986). Taxa with different taphonomic characteristics are likely to withstand different degrees of damage before becoming unidentifiable (e.g., Perry 1998), and therefore record different amounts of time-averaging even within the same sedimentary deposit. Differential time-averaging has important implications not only for the age model of the deposits but also for the creation of death assemblages and the formation of the fossil record.

Although the composition of molluscan death assemblages is largely consistent with the composition of the living shelled-mollusc community (Kidwell 2001), significant biases may be imposed by the preservational characteristics of individual organisms. Several studies have implicated body size as an important correlate with preservation potential (Kidwell 2002; Cooper et al. 2006), and previous analyses of *Tellina* documented significant differences between the half-lives of large and small shells (Kosnik et al. 2007). Shell thickness has been shown to be a good predictor of the resistance of a shell to breakage (Zuschin and Stanton 2001), and shell surface-area-to-volume ratios have been found to be important taphonomic predictors in laboratory dissolution studies (Flessa and Brown 1983; Glover and Kidwell 1993). Shell mineralogical composition including the organic content of the shell has also been shown to be important to shell survival (Glover and Kidwell 1993; Harper 2000; Best et al. 2007). Shell durability is an important, if difficult to quantify, property that significantly influences the taxonomic composition of all fossil-bearing sedimentary deposits.

Tropical carbonate systems are widespread and important, both in modern and in ancient times, yet most studies of molluscan time-averaging and taphonomy have examined shells from environments dominated by siliciclastic sediment (but see Carroll et al. 2003; Kidwell et al. 2005; Kosnik et al. 2007). Understanding the formation of modern carbonate deposits is important to our understanding of the evolutionary and ecological history of tropical marine systems including carbonate fossil deposits. Although Paleozoic benthic environments may have witnessed much lower levels of bioturbation (Bottjer and Ausich 1986), differences in shell durability are still likely to influence the formation of fossil deposits (e.g., Cummins et al. 1986). This study examines the differential time-averaging in typical mid-shelf Great Barrier Reef (GBR) lagoon-back reef sediments by dating shells from four molluscan taxa found in the top 125 cm of sediment.

Study Area and Material

Rib Reef is a typical central GBR mid-shelf reef (18.479°S,146.869°E; Fig. 1). The southern and eastern edges of the reef are well-developed reef crests sheltering a lagoon-back reef sedimentary wedge that slopes from ~5 to ~60 m below sea level over ~2 km distance from the reef framework. The sediment surface is exclusively wave marked in shallow water, but as water depth increases *Callianassa* (infaunal shrimp) burrows become increasingly common. Two large-diameter suction cores were collected in February and June 2005; core 1 was collected ~200 m NW of the reef framework at 6.7 m below the lowest astronomical tide datum and core 2 was ~60 m NW of core 1 in 7.1 m of water. A sheet metal tube 56 cm in diameter (0.25 m^2 surface area) was sunk into the lagoon sediment using the R/V *James Kirby's* vibrocore head. Sediment layers were removed from the interior of the tube in 5 cm intervals to a depth of ~130 cm below the sediment-water interface using a diver-operated airlift. Sediment was collected in ~1-mm-mesh bags.

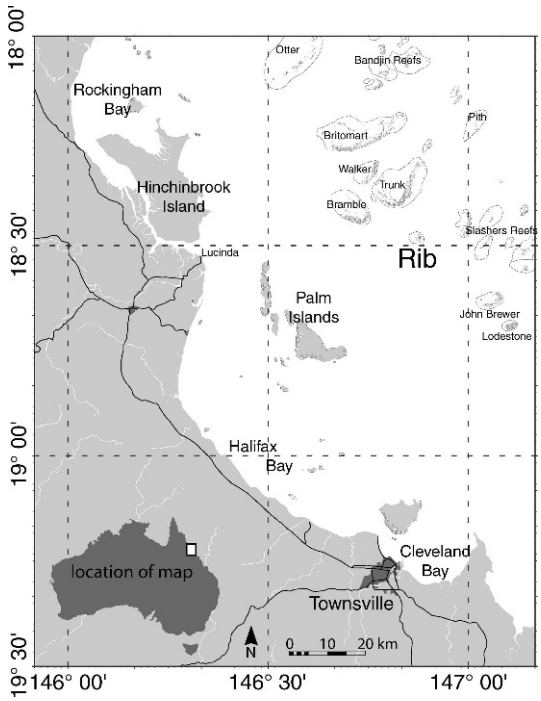

FIGURE 1. Map of the central Great Barrier Reef showing the location of Rib Reef. Map redrawn and simplified from the Great Barrier Reef Marine Park 2003 zoning plan map MPZ8 - Townsville.

Each layer was sieved through nested 4, 2, and 1 mm sieves, but only shells from the >4 mm sieve fraction were used in the analyses presented here. Shells from the >4 mm fractions of six layers were used from core 1: 5–10, 15–20, 50–55, 80–85, 110–115, and 120–125 cm. Shells from the >4 mm fractions of every third layer were used from core 2: 0–5, 15–20, 30–35, 45–50, 60–65, 75–80, 90–95, and 105–110 cm.

Four taxa were selected for dating: *Ethalia*, *Natica*, *Tellina*, and *Turbo*. These four taxa are well represented in these samples, and they span a range of robustness and life habits. These data were used to examine the effect of various options on the creation of calibration curves for amino acid geochronology (Kosnik et al. 2008) and the efficacy of various screening criteria and cutoffs (Kosnik and Kaufman 2008). Analyses of the *Tellina* data were published in Kosnik et al. (2007).

Ethalia.—Shells of *Ethalia guamensis* (Quoy and Gaimard 1834), an infaunal gastropod frequently found living in areas with actively bioturbated surface sediment, are common in the death assemblage of Rib Reef lagoon. Nearly all of the 64 *Ethalia* shells recovered were complete and in excellent condition, retaining a glossy luster and showing minimal abrasion or chipping (Fig. 2A,B). The body whorl of 56 shells from the Rib Reef cores was analyzed for amino acid racemization (AAR). Calendar ages were inferred from AAR calibration curves based on six accelerator mass spectrometry (AMS) ^{14}C ages (OZJ024–OZJ029) and four live-collected specimens. Specimens ranged in size (measured as the geometric mean of the three longest perpendicular dimensions) from 3.8 to 10.0 mm with a median value of 6.0 mm.

Natica.—The *Natica* shells recovered displayed a wide range of color morphs making species assignment difficult, but 62 of 148 specimens were assigned to a highly variable *N. gualtieriana* group on the basis of their two or three rows of vertically elongated spots arranged in spiral bands (Fig. 2C,D). Although recovered from the death assemblage in areas with actively bioturbated surface sediments, the infaunal gastropod *Natica gualtieriana* Récluz 1844 was found living only in areas stabilized by vegetation. Nearly all of the *N. gualtieriana* shells were complete, but some lacked their original glossy luster or had a chalky precipitate on the shell surface, and 23% (14 of 62) had predation drill holes. The body whorl of 52 shells from the Rib Reef cores was analyzed for AAR. Calendar ages were inferred from AAR calibration curves based on six AMS ^{14}C ages (OZJ012, OZJ019–OZJ023) and five live-collected specimens. Specimens ranged in size from 4.0 to 8.4 mm with a median value of 5.0 mm.

Tellina.—The mollusc species whose shells were most abundant, *Tellina (Pinguitellina) casta* Hanley 1844, was found living in areas with actively bioturbated sediment (Fig. 2E,F). Of the >2000 complete valves recovered, only right valves in good condition were analyzed to avoid contamination and to exclude the possibility of analyzing the same individual twice. The posterior halves of 245 right valves from the Rib Reef cores were analyzed for AAR. Calendar ages were

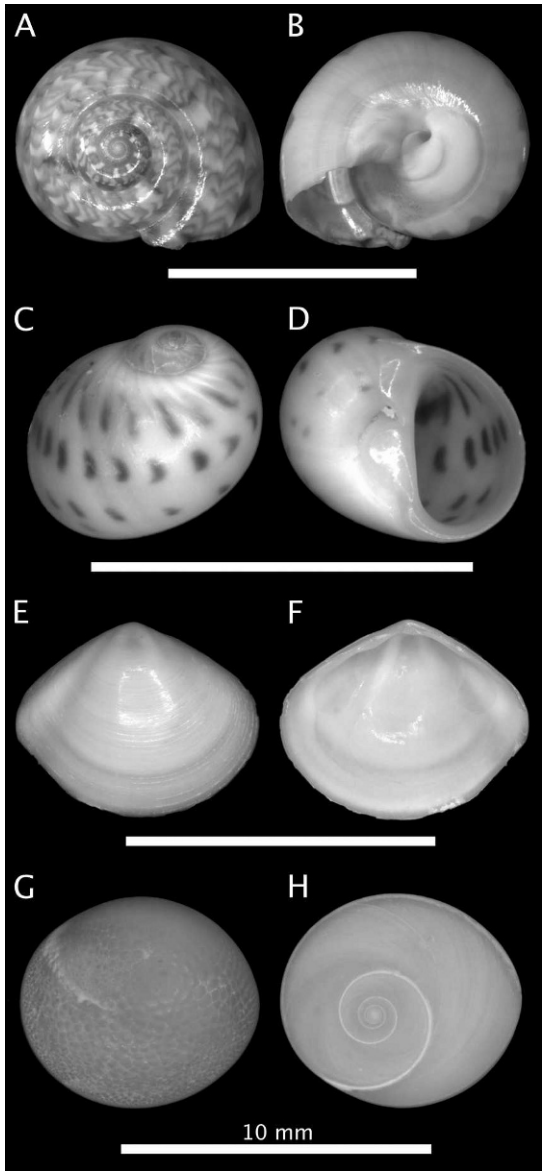

FIGURE 2. Images of the taxa used in this study. All scale bars, 10 mm. Photographed specimens are deposited at the National Museum of Natural History, Washington, D.C. A, B, *Ethalia* (USNM 1122320). C, D, *Natica* (USNM 1122321); E, F. *Tellina* (USNM 1122322). G, H, *Turbo* operculum (USNM 1122323).

inferred from AAR calibration curves based on 13 AMS ^{14}C ages (OZI199–OZI207, OZJ013–OZJ016) and six live-collected specimens. Specimens ranged in size from 2.9 to 8.3 mm with a median value of 6.0 mm.

Turbo.—*Turbo* opercula are dense calcium carbonate discs that plug the opening of the shell when the animal is retracted (Fig. 2G,H). Opercula are fairly common in Rib Reef lagoon sediments (172 recovered), but living *Turbo (Marmarostoma) argyrostomus* (Linnaeus 1758) are found exclusively on the reef framework where they graze on hard substrates and hide in crevices. Nearly all of the opercula were unbroken, but most showed signs of encrusting algae, microborers, or carbonate precipitate. *Turbo* opercula closely match the size and shape range of *Tellina* valves, but they are far more robust. The extent of AAR was determined for 98 disassociated opercula from the Rib Reef cores. Calendar ages were inferred from AAR calibration curves based on 11 AMS ^{14}C ages (OZI190–198, OZJ017, OZJ018) and on two opercula from live-collected specimens. Specimens ranged in size from 3.9 to 8.8 mm with a median value of 5.2 mm.

Methods

Shell Measurements.—All linear shell measurements were taken with digital calipers to 0.01 mm. Shell size was measured by taking three perpendicular measurements, the longest linear dimension (x), the next longest linear measurement perpendicular to the first measurement (y), and the length perpendicular to the first two measurements (z). Shell size was calculated as the geometric mean of x, y, and z (Kosnik et al. 2006). *Ethalia* and *Natica* shell thickness was measured by taking several measurements along the outer aperture edge to determine a representative thickness. *Tellina* shell thickness was measured by taking several measurements along the ventral shell edge to determine a representative thickness. As opercula lack a clear edge, *Turbo* shell thickness was the minimum shell dimension (z). Shell mass was measured using a digital balance to 0.01 mg.

Shell Size.—Shell size has been shown to affect durability and half-life. Kosnik et al. (2007) showed that small *Tellina* shells had shorter half-lives than large *Tellina*. Whereas those results demonstrated that size is important within taxa, the analyses here examine the importance of size in a multi-taxon context including differing shell density, thickness, or shape as defined below. Restricting the analysis to only core 2 where all

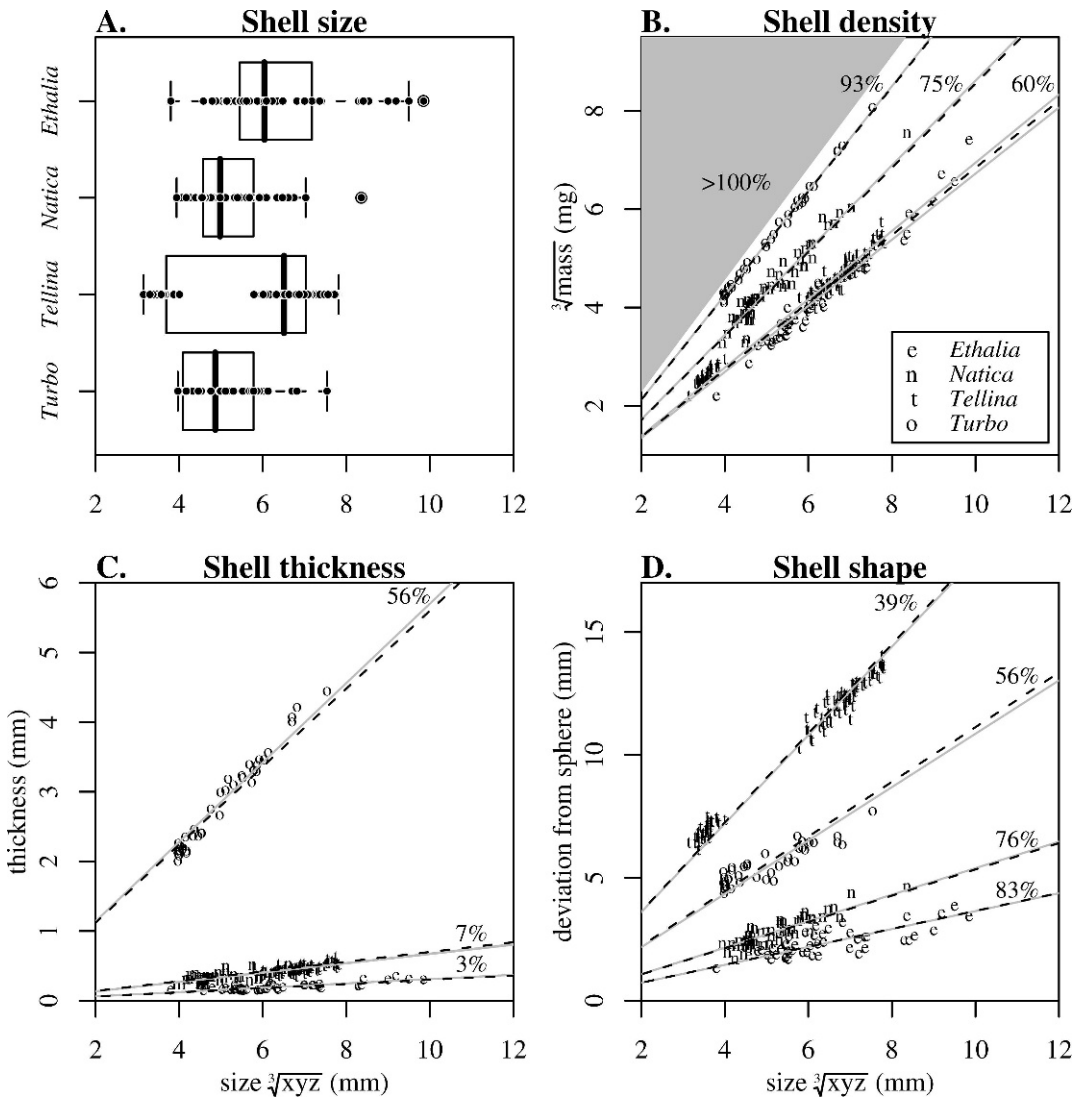

FIGURE 3. Morphological characteristics affecting durability. All panels have shell size (the geometric mean of the three longest perpendicular dimensions in mm) on the x-axis. A, Shell size by taxon with overlying boxplots indicating the median, quartiles, and extremes less than 1.5× the interquartile width. B, Shell density. Cube root of shell mass (mg) on the y-axis with shells from each taxon plotted using the symbols shown in the legend. Gray lines are best-fit relations, dashed lines are fixed proportions of solid calcite spheres, and the gray area indicates the area denser than aragonite. C, Shell thickness (mm) on the y-axis with the same plot symbols as B, but dashed lines are fixed proportions of shell size. D, Shell shape measured as the deviation from a sphere (mm) on the y-axis with the same plot symbols as B; dashed lines correspond to theoretical oblate spheres whose z measurement is X% of the size.

four taxa were sampled, *Tellina* should be the most durable (median size = 6.4 mm), followed by *Ethalia* (median size = 6.0 mm), and *Natica* and *Turbo* should be the least durable (median sizes of 5.0 and 4.9 mm respectively). Shell size shows more intra-taxon variability than any other durability metric examined here. In this data set, the size range within taxa is much greater than the size difference between taxa (Fig. 3A). Small *Tellina* were specifically sampled from alternate layers of core 2, and if size alone determined shell durability, small *Tellina* (median size = 3.55 mm) would be the least durable shells and large *Tellina* (median size = 6.88 mm) would be the most durable shells.

Shell Density.—All four taxa show strong linear relations between shell size measured

as the geometric mean of the three longest perpendicular dimensions and the cube root of shell mass. *Ethalia* and *Tellina* specimens were the lightest for their size (Fig. 3B). *Natica* shells were intermediate between *Ethalia*/*Tellina* and *Turbo* opercula, which were the heaviest for their size (Fig. 3B). These size-versus-mass relations can be more easily compared in the context of shell density. Although measuring shell volume is difficult, the size-versus-mass relation can be readily compared with the mass of an aragonite spheroid of the same size (same geometric mean of the three longest perpendicular dimensions) as the shells. This procedure yields an intuitive and size-independent value of relative shell density for each taxon with a theoretical range of 0 to 100%. A value of zero equates to the absence of a shell, and 100% is a solid aragonite spheroid (approaching 100% is unlikely if the organism's soft tissue is contained within the shell). Using relative shell density as a proxy for shell durability indicates that *Ethalia* and *Tellina* should be the least durable, with shell densities approximately 60% that of a solid spheroid (Fig. 3B). *Natica* shells should be intermediate, with a shell density approximately 75% that of a solid spheroid, and *Turbo* opercula should be the most durable, with a shell density 93% that of a solid spheroid (Fig. 3B). Because opercula do not house animals, their lack of internal habitable spaces results in a very dense shell.

Shell Thickness.—Thicker shells require more mechanical force to break (Zuschin and Stanton 2001), and they have less shell volume exposed to chemical dissolution than thinner shells of the same size and shape. Shell thickness has a strong taxon-specific linear relation with shell size, and these relations can be used to create a size-independent measure of shell thickness expressed as a proportion of shell size. *Ethalia* has the thinnest shell at 3% of shell size, followed by *Natica* and *Tellina* with shell thicknesses of 7% and *Turbo* with an operculum thickness of 56% (Fig. 3C). Shell thickness predicts that *Turbo* should be the most robust and *Ethalia* should be the least robust. *Tellina* and *Natica* should be slightly more robust than *Ethalia* but much less robust than *Turbo* opercula.

Shell Shape.—A sphere has minimal surface area exposed to chemical dissolution, and maximal cross-sectional area resulting in maximal breaking resistance. The deviation of a shell from a perfect sphere was calculated by summing the absolute deviation of each perpendicular dimension from a sphere with the same size:

$$\text{Deviation}_{\text{shape}} = |d - x| + |d - y| + |d - z| \quad (1)$$

where d is the diameter of the sphere and x, y, and z are the shell dimensions along three perpendicular axes. Because the shell and the sphere have the same geometric mean size, the diameter (d) is constrained to equal $(x \cdot y \cdot z)^{1/3}$. Most molluscs, and each of these taxa, deviate from a sphere primarily along a single axis, and a shell's deviation is readily compared with that of a theoretical oblate spheroid with a single shortened axis that is expressed as a proportion of their size. A shell's deviation from spherical has a strong taxon-specific linear relation with shell size, and these relations were used to describe a size-independent measure of shell shape using oblate spheroids where 100% is a sphere and 0% is a thin circular sheet. *Ethalia* is closest to spherical, with a deviation equal to that of an oblate spheroid with a single axis 83% of that of a sphere, followed by *Natica*, *Turbo*, and *Tellina* deviations, which are 76%, 56% and 39%, respectively (Fig. 3D). Shell shape indicates that *Ethalia* should be the most robust, followed by *Natica*, *Turbo*, and *Tellina*.

Shell Mineralogy and Microstructure.—Shell mineralogy and microstructure have been shown to be an important determinant of a taxon's fossilization potential (Harper 2000; Wright et al. 2003; but see Kidwell 2005). X-ray diffraction and X-ray fluorescence analyses confirmed that the mineralogical composition of the shells examined here is pure aragonite. Examination of shell surfaces and cross-sections using a scanning electron microscope (SEM) revealed that each taxon has a different shell microstructure. Although mineralogy and microstructure are likely to be important to the broader discussion of mol-

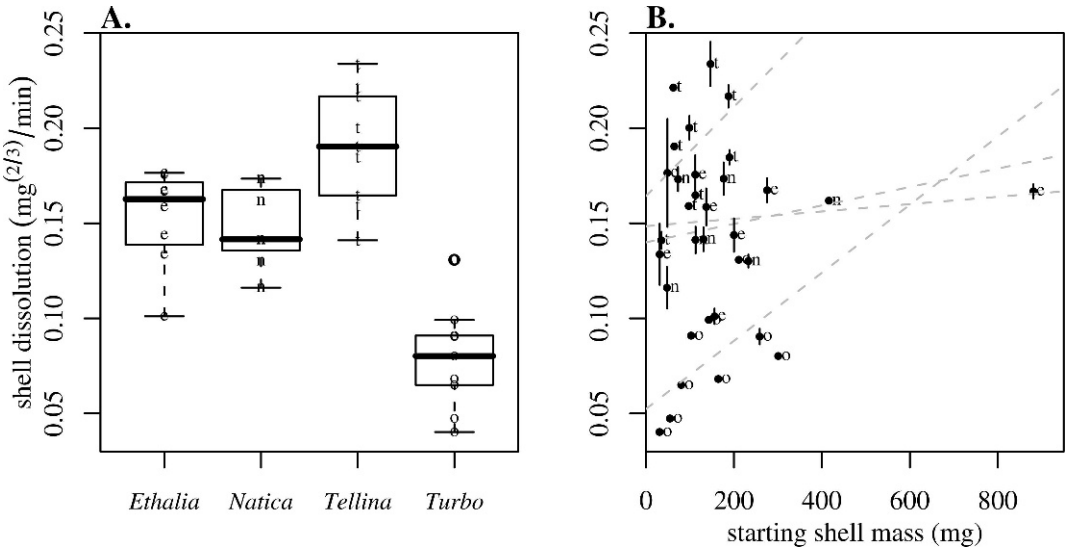

FIGURE 4. Summary of shell-dissolution experiments. The rate of shell loss ($mg^{(2/3)}$ / min) in 0.1 M HCl on the y-axis. A, Rate of shell loss by taxon. *Turbo* has the lowest rate of dissolution, and *Tellina* has the highest rate. B, Rate of shell dissolution versus the starting shell mass (mg) on the x-axis. None of dashed gray regression lines are statistically significant. *Ethalia* and *Natica* show no clear relation with starting mass. The apparent relations indicated for *Turbo* and *Tellina* are overwhelmed by within-taxon variability.

luscan preservation in carbonate sediments, they are beyond the scope of the present study.

Shell Dissolution.—Given the different predictions of shell durability generated by each morphological metric, and considering each taxon's distinct shell microstructure, an additional empirical measure of shell durability was sought. Although measuring physical breakage is complicated by a multitude of factors, a shell's chemical stability can be readily measured as the dissolution rate in an acidic solution. We experimentally dissolved shells in dilute HCl to measure their relative durability. This affords a relative index of chemical stability, but it is not intended to be equivalent to natural conditions in sedimentary environments.

Nine empty shells from each taxon were selected to cover the observed size range. Dry shells were weighed, etched for 30 min in 0.1 M HCl with manual agitation every 30 sec, rinsed with distilled water, dried overnight at 55°C, and reweighed. This process was repeated until the shell was dissolved. Shell mass is a function of shell volume, whereas dissolution rate should be a function of shell surface area. Therefore, shell mass raised to the 2/3 power should be linearly related to the time in acid. Regression models were fit to determine the rate of shell loss (the slope of the $mass^{(2/3)}$ versus time in acid).

The results show that the rate of shell loss is taxon dependent (Fig. 4A). *Turbo* has the lowest rate of shell loss, whereas *Tellina* has the highest rate, with *Ethalia* and *Natica* intermediate. The rate of shell loss is not a function of the original shell mass (Fig. 4B). *Ethalia* and *Natica* show no relation between starting shell mass and the rate of loss, and the apparent relations shown by *Tellina* and *Turbo* are not statistically significant because of high variability within the taxa (*Tellina* $p > 0.26$, *Turbo* $p > 0.08$, Fig. 4B). Although the shells used in this experiment reflected the specimen sizes found in these core samples, significantly larger *Turbo* opercula have been found in other sediment samples. With the addition of larger *Turbo* opercula, it may be found that larger opercula dissolve faster than smaller opercula, but the increased initial shell mass would negate the increased rate of shell loss (e.g., the time to complete shell loss would still be longer for larger shells). None of the other taxa are likely to be

TABLE 1. Taxon specific AAR calibration curve parameters for aspartic and glutamic acid. These parameters define a line ($y = m(D/L)^x + b$) relating the extent of AAR to shell age. Shell age before A.D. 1950 (y) is determined by the slope of the relation (m), the D/L exponent (x), and the y-axis intercept (b). In these calibrations b is constrained to be the year the live-collected specimens were collected (A.D. 2005 or 2006). Abbreviations: n, the number of subsamples used to fit the calibration curve; r^2, the fit of the calibration curve; Min and Max, the minimum and maximum calibrated ages in years before A.D. 1950. Asp and Glu D/L values for each shell's subsamples are presented in the supplemental online material.

Taxon	Amino acid	n	b	m	x	r^2	Min	Max
Ethalia	Aspartic	12	−56	19452	3.46	0.99	−56	3354
	Glutamic	12	−56	49066	1.99	1.00	−56	3363
Natica	Aspartic	12	−56	19320	3.19	0.99	−56	3694
	Glutamic	12	−56	60191	2.24	0.99	−56	3855
Tellina	Aspartic	26	−55	37709	2.54	0.98	−55	4751
	Glutamic	26	−55	55577	1.78	0.98	−55	4611
Turbo	Aspartic	20	−55	17217	3.51	0.88	−55	3741
	Glutamic	20	−55	28703	1.61	0.91	−55	4401

represented by individuals larger than those dissolved in this experiment.

Determining Shell Age.—Shell ages were determined from quasi-independent taxon-specific amino acid racemization calibration curves for aspartic and glutamic acid. A calibration curve was developed for each amino acid using a simple power-law transformation, where D/L was raised to the best-fit exponent, the origin was constrained by the D/L value of live-collected specimens, and the ^{14}C ages were weighted by their 2σ calibrated age ranges (Table 1) (Kosnik et al. 2008). The AAR data from duplicate subsamples of each shell were screened using the procedures examined in detail by Kosnik and Kaufman (2008). Any subsample with age estimates inferred from the two amino acids that differed by ≥200 yr or by ≥20% relative to the mean inferred age was removed from the data set. The subsamples meeting this criterion (i.e., $Y < 0.2$) were averaged to determine the specimen age used in these analyses. In all, 17 specimens (4%) without subsamples meeting this criterion were excluded from the analyses. As a result, the variability of D/L values in some taxa was reduced (see Kosnik and Kaufman 2008 for further discussion on the rationale behind the data screening and the effect of the procedure on the overall geochronological results). Following these procedures, the mean age error (1σ) for individual shells based on two amino acids analyzed in duplicate subsamples ranged from 53 to 142 yr for *Tellina* and *Turbo*, respectively. The $Y < 0.2$ data set used here includes 51 *Ethalia*, 51 *Natica*, 245 *Tellina*, and 81 *Turbo* specimens. Specimen ages are presented as calendar years before A.D. 1950 (B.P.) unless otherwise noted. AMS radiocarbon dating was carried out at the Australian Nuclear Science and Technology Organisation and AAR analyses were performed at Northern Arizona University. Technical details of these analyses can be found in Hua et al. (2001) and Kaufman and Manley (1998), respectively. The ^{14}C and D/L data used in calibration are presented in the supplemental online material at http://dx.doi.org/10.1666/08060.s1.

Shell Half-Lives.—Shell half-lives derived from an exponential distribution fit to the age-frequency distribution can be used to determine the rates of shell destruction (e.g., Cummins et al. 1986; Meldahl et al. 1997). Assuming stochastically constant shell input and neutral horizontal movement allows us to use half-lives as a measure of two processes: (1) the vertical movement of shells out of the sampled layer; or (2) the destruction of the shells. Exponential distributions were fit and bootstrapped using the ''fitdistr'' and ''boot'' functions in R (see below). Exponential distributions are defined only for positive values, so AAR ages were rescaled to set A.D. 2006 equal to zero yr (the collection date) before fitting the distributions and calculating half-lives.

Statistical Treatment.—All statistics, data manipulation, and plotting were done using R 2.8 for Mac OS X (R Development Core Team 2008). In addition to the R core, extensive use was made of the MASS 7.2-45 (fitdistr), and boot 1.2-34 (boot) packages.

Results

Shell Age and Burial Depth

Although the carbonate sediment of central GBR mid-shelf reef lagoons is visually homogenous, extensive coring consistently has

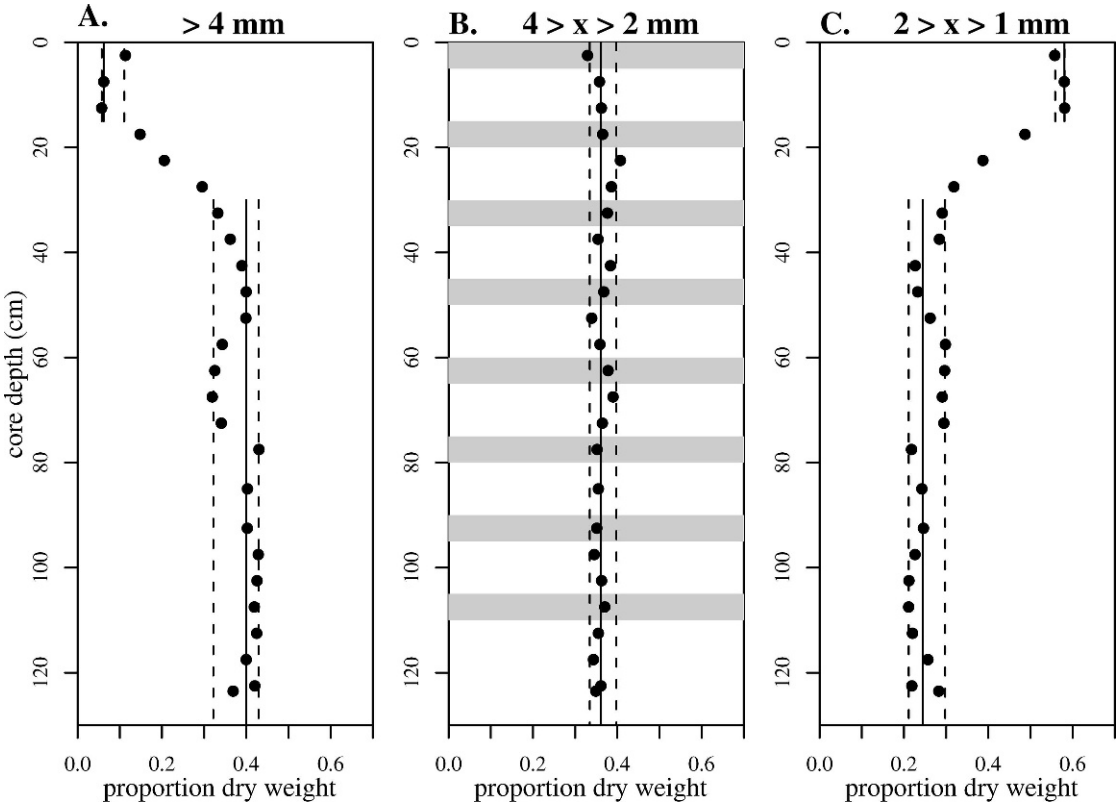

FIGURE 5. Sediment grain size from core 2 illustrating a marked coarsening of sediments below 30 cm, expressed as a proportion of each layer's dry weight. Solid vertical lines are the median proportions for the surface layer (0–15 cm) and the deeper layer (30–120 cm), and the dotted lines are 95th quantiles. A, Sediments from the >4 mm sieve fraction are more abundant in the deeper layer than the surface layer. B, Sediments from the <4 mm and >2 mm sieve fraction represent a consistent proportion of the sample layers; gray bars indicate the sedimentary layers from core 2 from which specimens were taken for this study. C, Sediment from <2 mm and >1 mm sieve fraction is far more abundant in the surface layer than in deeper layers.

found that the upper 20 cm of the sediment column contains more fine particles than deeper sediments, and nearly all of the very large (>4 mm) material in the upper 20 cm is living (Kosnik and Wüst personal observation). The proportion of sediment mass >1 mm in each sedimentary layer shows a marked increase in coarse grains between core depths of 15 and 30 cm (Fig. 5). Below 30 cm, the >4 mm sieve fraction made up 40% of each layer's dry mass whereas above 15 cm the >4 mm sieve fraction made up only ~10% of each layer's mass (Fig. 5A). The 2–4 mm fraction consistently constituted ~35% of each layer's mass through the entire core (Fig. 5B). The increase in >4 mm material was offset down-core by the 1–2 mm sieve fraction; it constituted nearly 60% of each layer's mass above 15 cm, but only about 25% of each layer's mass below 30 cm (Fig. 5C).

This particle size division was mirrored in the *Tellina* age structure; valves from the top 20 cm of both cores were significantly younger than valves from deeper layers (Kruskal-Wallis $p < 0.01$, Figs. 6A, 7C). *Ethalia* shells in core 2 also suggested a division, but the sample size was insufficient to draw strong conclusions ($p = 0.06$, Fig. 7A). No *Natica* shell was recovered from the top 20 cm (Fig. 7B). *Turbo* opercula had a homogeneous age distribution through the entire sediment profile in core 1 ($p = 0.19$, Fig. 6B), but no opercula were recovered from the upper 20 cm of core 2 (Fig. 7D). Because *Turbo* live on hard substrates, the opercula found in surface sediments must be transported from the nearby reef matrix. The time required for

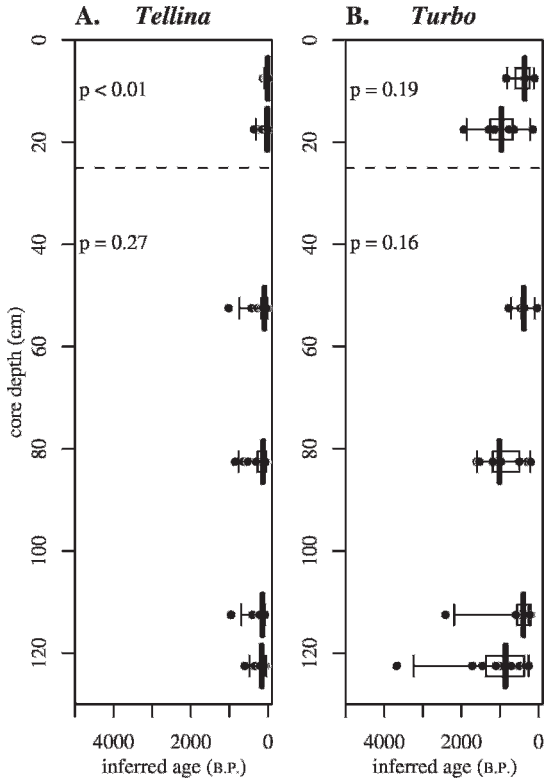

FIGURE 6. Shell age and depth from core 1. Shell age in calibrated years since A.D. 1950 on the x-axis and core depth in centimeters on the y-axis. Individual shells are plotted as circles, and layers are overlain with boxplots indicating the median age (vertical line), quartiles (box), and 95th quantile (whiskers). A dashed line at 25 cm separates the upper ''surface layer'' from the lower ''deep layer.'' Two Kruskal-Wallis *p*-values are indicated; the upper *p*-value tests all sampled layers, and the lower *p*-value tests only layers deeper than 25 cm. A, *Tellina* valves. The samples from the upper layer are younger than deeper layers, but deeper layers are homogeneous. B, *Turbo* opercula. All of the layers are age homogeneous.

this movement may result in a lag in operculum supply and account for both the relatively older shells in the surface sediments and the resulting lack of an age disjunction down-core. The age of *Turbo* opercula in surface sediments indicates that this movement may be quite slow. In addition to age distributions, molluscan shell abundance increases markedly below 25 cm, suggesting that shells are concentrated in the deeper sedimentary layer.

Excluding shells from the top layer (<25 cm), none of the taxa in either core show a down-core increase in age, and there is no support for age differences between layers ($p \geq 0.14$, Figs. 6, 7). Some of the youngest shells of each taxon are found in the deepest layers, while some of the oldest shells of most taxa are found in the top half of the core (e.g., above 65 cm). Shells between 25 and 125 cm depth are sufficiently mixed to homogenize each taxon's age distribution. Rates of sediment turnover are sufficient to transport shells ~50 yr old to 120 cm depth. In the 30–35 cm layer of core 2 the oldest shells were 2213, 1148, 4670, and 1258 B.P. for *Ethalia*, *Natica*, *Tellina* and *Turbo*, respectively. Below 100 cm the youngest shells are 580, 74, 50, and 304 B.P. for *Ethalia*, *Natica*, *Tellina*, and *Turbo*, respectively. The dated shells buried between 25 and 125 cm are an age-homogeneous assemblage accumulated over the past ~4600 yr.

Shell Durability and Survival

Shell size, density, thickness, and shape as predictors of shell durability and half-life were compared with the observed shell half-lives of the four taxa. These analyses included only specimens from below 20 cm to avoid mixing distinct specimen age-populations.

Comparing Cores.—The cores show distinct results for the two taxa dated from both cores. In core 1, the *Tellina* half-life was 171 yr, and the *Turbo* opercula half-life was 552 yr (Fig. 8). In core 2, *Tellina* half-life was 574 yr (Fig. 9C), and *Turbo* opercula half-life was 1229 yr (Fig. 9D). In core 1, the *Turbo* opercula had a half-life more than three times longer (4.2×) than that of *Tellina* shells, whereas in core 2 the difference was only just over twofold (2.1×). Core 2 contained an older shell assemblage and yielded longer shell half-lives than core 1. There was no difference in *Tellina* size or mass (Wilcox $p = 0.14$, $p = 0.21$) across cores, but *Tellina* shells in core 2 had a half-life 4.4 times as long as *Tellina* from core 1 (Figs. 8A, 9C). *Turbo* opercula in core 2 had a half-life 2.2 times that of *Turbo* opercula in core 1 (Figs. 8B, 9D) despite being significantly smaller ($p = 0.02$, median size in core 2 = 4.76 mm, median size in core 1 = 5.43 mm) and lighter ($p = 0.01$, median mass in core 2 = 123 mg, median mass in core 1 = 199 mg) than opercula in core 1. The large differences between cores illustrate fine-scale spatial

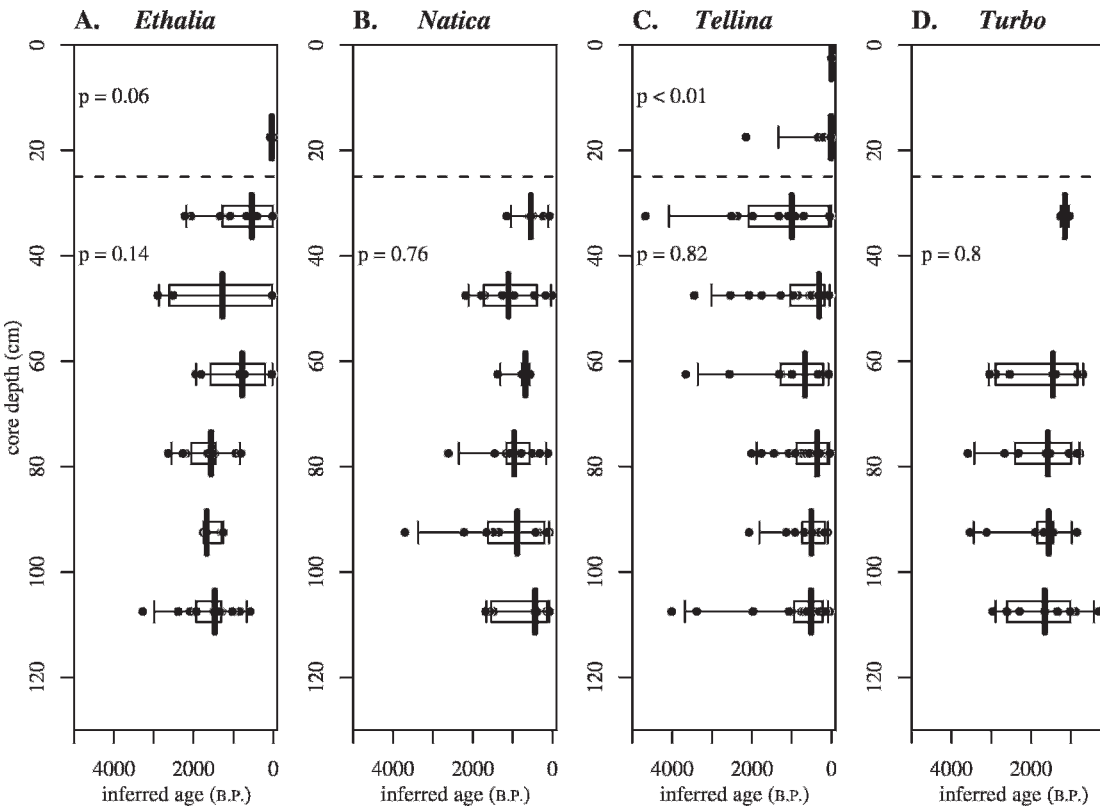

FIGURE 7. Shell age and depth from core 2. Plot format is the same as Figure 6. A, *Ethalia* shells. Although no sample is significantly different, shells from upper layer are essentially modern. B, *Natica* shells. None was recovered from the upper layer, but the deeper layers are age homogeneous. C, *Tellina* valves. Shells from the upper layer are younger than deeper layers, but the deeper layers are age homogeneous. D, *Turbo* opercula. None was recovered from the upper layers, but the deeper layers are age homogeneous.

heterogeneity in the degree of time-averaging and shell half-lives within modern tropical carbonate lagoons, and it also suggests significant spatial variation in taphonomic processes. The *Turbo* assemblage from core 1 has a half-life comparable to the half-lives of *Tellina* and *Natica* from core 2, rather than a half-life comparable to *Turbo* from core 2. *Turbo* variability between cores 1 and 2 exceeds taxonomic variability seen within core 2.

Judging from the generally younger shell population and shorter half-lives, the shells in core 1 appear to have been subjected to harsher conditions than the shells in core 2.

Comparing Taxa.—In core 2, *Tellina* and *Natica* had the shortest half-lives at 574 yr and 630 yr respectively (Fig. 9B,C). The *Ethalia* half-life was significantly longer at 925 yr (Fig. 9A), and *Turbo* opercula half-life was even longer at 1229 yr (Fig. 9D). This order was substantially different than the order suggested by increasing (1) shell density (*Tellina*/*Ethalia* < *Natica* < *Turbo*), (2) shell thickness (*Ethalia* < *Tellina*/*Natica* < *Turbo*), (3) shell shape (*Tellina* < *Turbo* < *Natica* < *Ethalia*), (4) median shell size (*Turbo* < *Natica* < *Ethalia* < *Tellina*), or (5) median shell mass (*Ethalia* < *Natica* < *Tellina* < *Turbo*) (Table 2). Shell size and mass were strongly related and highly variable within taxa (Fig. 3A), whereas the other three characteristics (i.e., density, thickness, and shape) were consistent within taxa (Fig. 3B–D).

Averaging the three morphological characteristics that were consistent within taxa to create a mean durability score resulted in a sequence (*Tellina* < *Ethalia/Natica* < *Turbo*; Table 2) more similar to the sequences observed for half-lives (*Tellina*/*Natica* < *Ethalia*

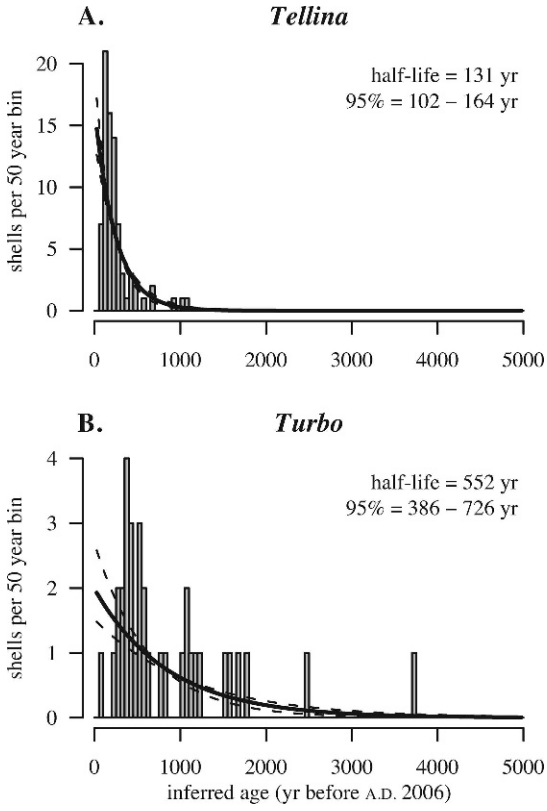

FIGURE 8. Age-frequency distributions overlain with best-fit exponential distributions from core 1. Only shells recovered from deeper than 25 cm are included. Shell half-lives with 95% bootstrapped confidence intervals. Shell age relative to A.D. 2006 on the x-axis, and 50-yr histogram bins. A, *Tellina*. B, *Turbo* opercula.

< *Turbo*; Fig. 9) and experimental dissolution rates (*Tellina* < *Ethalia/Natica* < *Turbo*; Fig. 4A) than for those of any of the individual durability metrics.

Although a durability score of zero is expected to have a half-life of zero there is no such a priori expectation for shell dissolution rate. Given the different half-lives between cores, these taphonomic relations are expected to be site-specific, but these relations explicitly predict the half-lives of the other aragonitic molluscan shells at these sites. Core 1 with only two taxa is plotted for comparison with core 2. Shell half-life has a strong relation to the mean durability score (Fig. 10A). Shell half-life has a weaker relation to the shell dissolution rate (Fig. 10B). These two hypothesized relations have slightly different implications for inferring shell durability. The

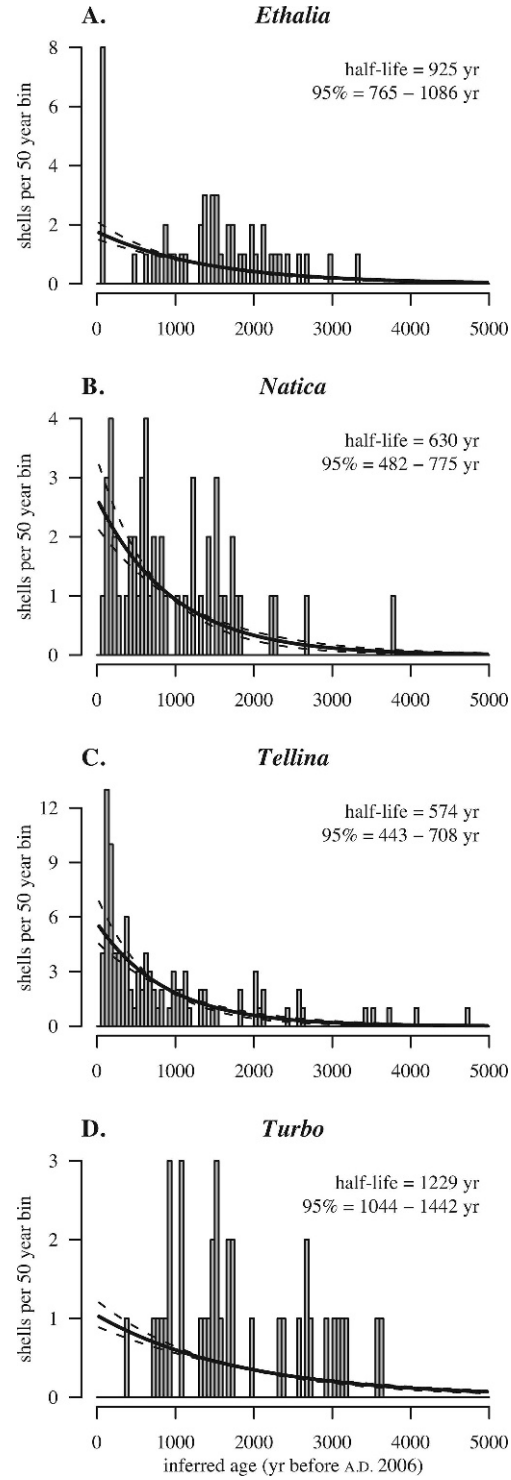

FIGURE 9. Age-frequency distributions overlain with best-fit exponential distributions from core 2. Only shells recovered from deeper than 25 cm are included. Plot format identical to Figure 8. A, *Ethalia*. B, *Natica*. C, *Tellina*. D, *Turbo* opercula.

TABLE 2. Summary of durability predictor variables. Median mass and size values are based only on shells from core 2 layers deeper than 20 cm. All of the specimens were used to calculate relative shell density, thickness, and shape.

	Median		Relative			
Taxon	Mass (mg)	Size (mm)	Density	Thickness	Shape	Mean score
Ethalia	63.19	6.07	0.60	0.03	0.83	0.49
Natica	83.18	4.93	0.75	0.07	0.76	0.53
Tellina	89.34	6.37	0.60	0.07	0.39	0.35
Turbo	133.31	4.76	0.93	0.56	0.56	0.68

mean durability score's zero intercept implies that the slope of the line defining the taphonomic relation should vary between sites (Fig. 10A), whereas the shell dissolution relation is not constrained by theoretical x- or y-intercepts and the data here suggest that the slope of the line defining the taphonomic relation does not change between sites (Fig. 10B). Although it should not be possible for shells with a durability score of 0 to have a half-life >0, it is possible that shells with a durability score >0 might still have a half-life that is effectively 0. The dashed gray line in Figure 10A suggests that shells from core 1 with a durability score <0.2 have effectively 0 half-lives. At this time the relations in Figure 10 should be considered hypotheses deserving additional study, and only additional data will be able to characterize the relation between shell durability and shell half-life. However, this approach provides a potential framework for examining this relation.

Examining the Effect of Shell Size.—Small *Tellina* were sampled from alternate layers of core 2 to examine the effect of shell size on half-lives, but the other taxa were not sufficiently abundant to implement a size-sensitive sampling procedure. In contrast to the bimodal distribution of *Tellina* shell size (<~4 or >~6 mm), the other taxa do not form distinct size classes (Fig. 3A). Instead, the other three taxa were divided into two equal data sets separated by the median shell size, and the half-life of each subset was determined. In all taxa, the small shells had a shorter half-life than the large shells, although bootstrapped confidence intervals for the two size classes overlap for *Ethalia* and *Natica* (Fig. 11A–D). Small *Tellina* have half-lives

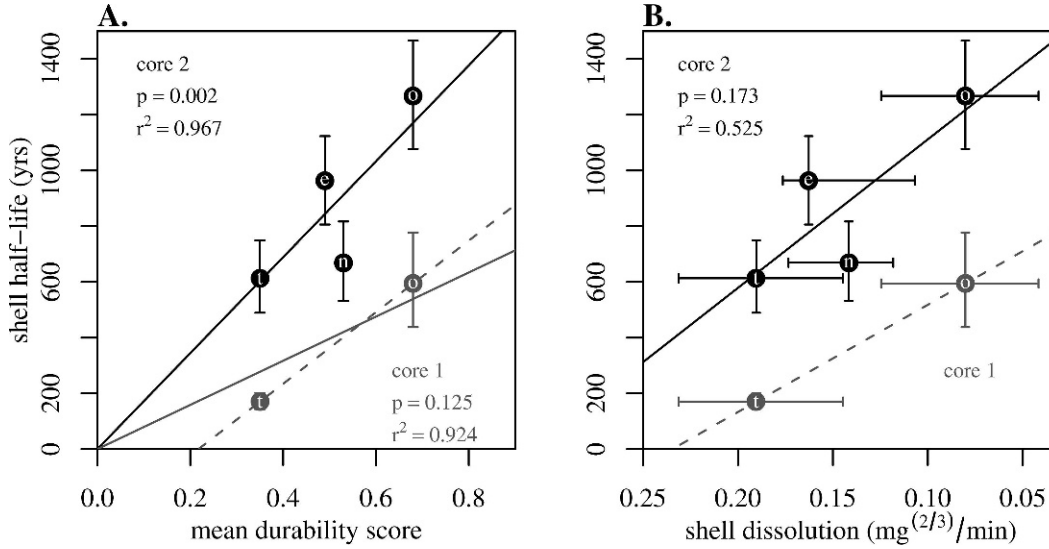

FIGURE 10. Shell half-lives as a function of durability predictors. Points are labeled using the legend from Figure 3; vertical error bars are the 95% bootstrapped confidence intervals (Figs. 8, 9). A, Shell half-life versus combined durability score with a regression line forced through the origin. B, Shell half-life versus rate of shell loss in acid dissolution experiments; horizontal error bars are 95% quantiles (Fig. 4A).

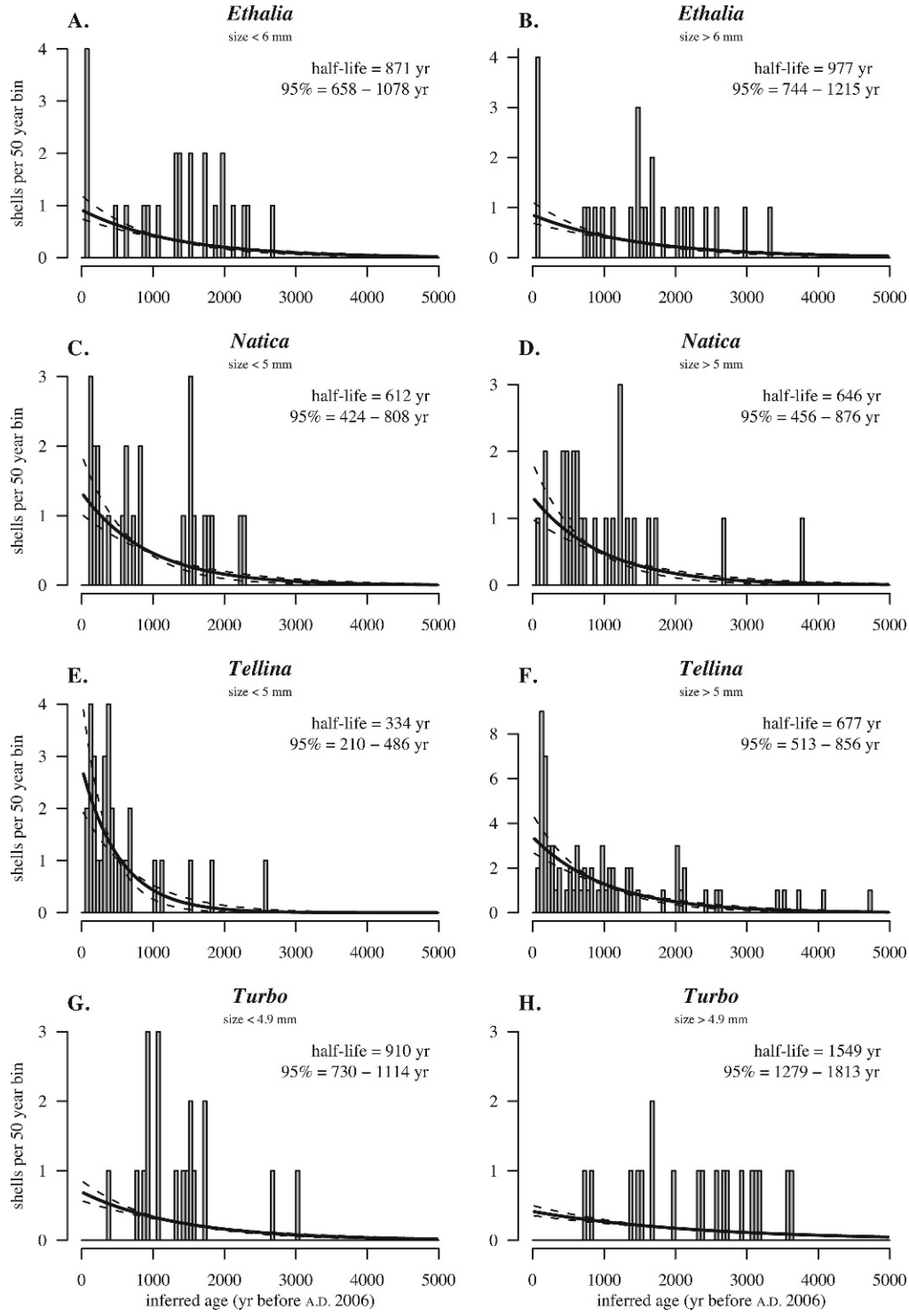

FIGURE 11. Shell size and half-life. Age-frequency distributions overlain with best-fit exponential distributions using shells recovered from deeper than 25 cm in core 2. The left column contains shells smaller than the median, whereas the right column contains shells larger than the median except in the case of *Tellina* for which small and large shells were specifically sampled. Plot format identical to Figure 8. In all cases the small shells have a shorter half-life than the large shells, but this difference is significant only for *Tellina* and *Turbo* opercula.

that are half that of large *Tellina* (334 versus 667 yr, Fig. 11E,F). Small *Turbo* opercula have significantly shorter half-lives than large opercula (910 versus 1549 yr, Fig. 11G,H). Although the data here are insufficient to quantify the effect, half-life is expected to vary with shell size. The difference between small and large *Ethalia* (5.5, 7.2 mm) and *Natica* (4.6, 5.8 mm) was less than the difference between small and large *Tellina* (3.6, 6.9 mm) and *Turbo* (4.1, 5.8 mm).

Greater differences between the size of small and large shells, or larger sample sizes for *Ethalia* and *Natica*, may reveal a relation between shell size and half-life. Notably, the shell dissolution experiments did not show size-specific rates of dissolution, but larger shells start with more mass to lose so if shells dissolve at the same rate larger shells will have longer half-lives. The dissolution experiments suggest that larger *Tellina* and *Turbo* might have faster rates of dissolution, but there was no such suggestion for *Ethalia* and *Natica*. This may be related to the simple scaling of *Tellina* and *Turbo* shell surface-area-to-volume ratio with size versus the relatively complex relation between surface-area-to-volume ratio and size when additional whorls are added to *Ethalia* and *Natica* shells.

Discussion

Burial and Bioturbation.—Callianassid shrimp have a well-documented bioturbation impact on coastal sedimentary environments mainly through effective particle sorting, such as the preferential burial of gravel-sized grains (Tudhope and Scoffin 1984; Tudhope 1989; Meldahl 1987; Bradshaw and Scoffin 2001). Because shell microborers are most active at the sediment-water interface, rapid burial promotes shell survival (Tudhope and Scoffin 1984; Perry 1998; Bradshaw and Scoffin 2001; Best et al. 2007). Following the death of an infaunal individual (here, *Ethalia*, *Natica*, or *Tellina*) its shell may never be exposed to the sediment-water interface, as it is likely to be buried rapidly below 20 cm (Figs. 6A, 7A,C) (Tudhope and Scoffin 1984; Tudhope 1989; Meldahl 1987; Bradshaw and Scoffin 2001). Although some studies (e.g., Bradshaw and Scoffin 2001) described this depth as near the base of the taphonomically active zone (TAZ, sensu Davies et al. 1989; Olszewski 2004), the shell ages presented here make that less certain. Certainly the top ~20 cm are distinct from the deeper layer, and the top layer is the taphonomically *most-active* zone; however, the homogeneous age distribution between 20 and 125 cm suggests that these shells are not below the depth of final burial (DFB, sensu Olszewski 2004). Indeed, Olszewski (2004) demonstrated the importance of non-coincident depths to define the TAZ and DFB. The data presented here do not directly address shell movement within the deeper sedimentary layer. It is possible that shells are transported directly from the surface layer to various depths within a callianassid burrow system, or that shells are repeatedly moved within this deeper sedimentary layer. Although the ages for >4 mm shells are consistent with movement within the deeper sedimentary layer, they also suggest that it is very unlikely for shells from the deeper layer to return to the top 20 cm. The distinct age distributions and half-lives of small versus large *Tellina* and *Turbo* suggest that the delineation of the TAZ and DFB is size dependent in these lagoonal sediments.

These findings are consistent with those of Tudhope and Scoffin (1984) who examined particle movement by callianassid shrimp in the Davies Reef (central GBR) lagoon. They found that while tagged sediment finer than 1–2 mm was generally ejected from the burrow and maintained in the surface layer, tagged sediment coarser than 1–2 mm was generally transported to depths between 20 and 60 cm. Tudhope and Risk (1985) suggested that the surface layer of callianassid-burrowed sediment is doomed to destruction, and it is the deeper layer that is likely to be preserved. Our work with individually dated particles corroborates this, showing that the top ~25 cm of sediment from central GBR lagoons has a different size composition and much younger shell age distribution than the underlying sediment that is more likely to be preserved in the fossil record. The activities of callianassid shrimp promote the burial and survival of coarser sedimentary material at

the expense of finer sedimentary material and fine-scale temporal resolution.

Stratigraphic Disorder.—The ultimate limitation to sampling resolution for sedimentary-based studies of ecology, evolution, and geochemistry is imposed by the sediments themselves. To be useful the scale of time-averaging in the sedimentary deposit cannot exceed the scale of the process being investigated (Kowalewski 1996). Sampling finer than the scale of time-averaging will not improve temporal resolution. Sedimentary deposits can be complete (in the sense that the entire time interval is represented), but still be mixed to a temporal scale coarser than required for a particular study (Flessa et al. 1993). Although increasing the number of ages per sedimentary layer will reduce the impact that rare shells have on the age of a particular layer (Cutler and Flessa 1990), sedimentary deposits such as those examined here are age homogeneous throughout the length of the core for most taxa given their occurrence frequency in the sediment. The four taxa examined here are among the most abundant in central GBR lagoonal sediment, and the sample volume was significantly larger than for traditional cores, yet the age distributions were homogeneous over the 125 cm length of the cores. The >4 mm fraction from these sediments is not suitable for examination of processes occurring on scales less than thousands of years, and the vertical distance between stratigraphic samples must exceed 1 m to detect significant differences in sample age. Similar findings of stratigraphic disorder were presented by Flessa et al. (1993), and the sedimentary depth at which shells became age stratified was not reached in either study.

Previous coring of similar reef sediments with a 76-mm-diameter vibrocore reached depths of 4 m (John Brewer Reef; Walbran et al. 1989), and 75-mm-diameters cores driven by hydraulic jackhammers reached depths of 7.5 m (Davies Reef; Tudhope and Scoffin 1984). Deeper coring could reveal the onset of age-stratified or additional age-homogeneous sediments. In central GBR mid-shelf lagoonal sediments, callianassid shrimp burrows have been recorded to depths of at least 60 cm (Tudhope and Scoffin 1984), and ^{210}Pb data suggested sediment mixing to over 1 m (Walbran 1996). Although our examination of the >4 mm fraction found a distinct top layer and a deeper age-homogeneous layer, Walbran et al. (1989) found stratigraphic consistency in the age of the bulk carbonate sediments from comparable water depths on a neighboring reef (John Brewer Reef, Walbran et al. 1989: Fig. 4). Despite the fact that ^{210}Pb is associated with finer sediment fractions, ^{210}Pb data from John Brewer Reef indicate an actively mixed layer from 0 to ~50 cm (with activity peaking at 19–22.5 cm) and a less actively mixed region from 50 cm to just over 1 m (Walbran 1996). Although the age of shells and the sediment containing them need not agree (e.g., Kershaw et al. 1988), greater understanding of size-biased bioturbation and preservation will ultimately be key to understanding these apparent contradictions in sedimentary records. The data presented here should emphasize the importance of performing paleontological analyses on the same individuals that are dated, and therefore the utility of the AAR approach, which affords a cost-effective means of dating hundreds of individuals.

Mineralogy and Chemistry.—Chemical processes are important in the creation of sedimentary deposits and fossil preservation. Although the loss of aragonitic shell material has been well documented in the fossil record (e.g., Wright et al. 2003), there is compelling evidence to suggest that an aragonite-calcite dichotomy is overly simplistic and that shell microstructure plays a pivotal role in shell durability (Glover and Kidwell 1993; Harper 2000; Best et al. 2007). Rapid dissolution and re-precipitation occurs in modern carbonate environments (e.g., Walter and Burton 1990; Patterson and Walter 1994; Sanders 2003). Therefore, the chemical stability of shell material is important to its ultimate survival even after it is buried, even in pure carbonate sediments where the pore-water chemistry promotes dissolution deep within the sediment (Walter and Burton 1990). Dissolution rates are likely to be higher where bioturbation is extensive and the sediments are relatively coarse. Although the pore-water

chemistry of central GBR sediments remains unstudied and studies from other areas have focused on the top meter, shell mineralogy and microstructure are likely to be important to the long-term survival in these sediments.

Although each taxon in this study has a distinct microstructure, all four taxa are entirely aragonitic. A durability score combining shell density, thickness, and shape yields results similar to those of the acid dissolution experiment. These data suggest that the differences in shell microstructure do not play a dominant role in determining the different half-lives of these four taxa in this environment.

Shell Half-Life.—Shell survival has been measured using a variety of methods including experimental deployments and dating shell assemblages, and each method has its strengths and weaknesses. Experimental shell deployments fixed at or above the sediment-water interface provide maximum opportunity for encrusting and bioeroding organisms to alter the shells, but as a consequence these deployments are difficult to compare with shells in the sediment. Experimental shell deployments on tethers or in bags have ''cage effects'' as individual shell movement is restricted within the sediment with possibly important restrictions on important taphonomic processes such as bioturbation. Fitting exponential distributions to dated shells to determine half-lives requires a series of assumptions that are certainly false. Shell input is unlikely to be constant, owing to years with ''high'' or ''low'' recruitment and/or survival. The probability of shell destruction is not age independent, as shell damage accrues over time and shell structure decays over time. But although older shells are likely to be more fragile than younger shells, studies have generally not found a significant relation between shell age and taphonomic condition (e.g., Meldahl et al. 1997).

Mollusc shell age distributions have been documented for several taxa and environments. These data have been treated somewhat differently, so to maximize comparability we have recalibrated radiocarbon ages published before the establishment of the consensus curve (Stuiver et al. 1998) using the calibration curve of Hughen et al. (2004), and we recalculated shell half-life using the curve-fitting functions of R to find the best-fit exponential curve. The original and recalculated data are recorded in Table 3 and supplemental online material. These studies should yield accurate half-life estimates for the shell population from which they were randomly sampled. Where ^{14}C ages were $\leq$1950 A.D., an age of 0 B.P. was used in the half-life calculation. The treatment of ''modern shells'' has a significant effect on the calculated half-life, but assuming an age of 0 B.P. was more justified than assigning ages between the date of publication and 1950 A.D. Excluding modern shells would result in a nonrandomly sampled shell population. Assigning ages in between the date of publication and 1950 A.D. would add an additional layer of assumptions to the calculations. This decision leads to slightly shorter half-lives than assigning the shells an age based on the date of publication. Only studies of shells collected from single localities were included.

Most studies are from the subtropical Gulf of California where *Chione* spp. valves collected at the sediment surface have half-lives that vary from 18 to 559 yr depending on the siliciclastic environment from which the shells were collected (Table 3) (Flessa et al. 1993; Martin et al. 1996; Meldahl et al. 1997). *Chione* spp. buried in marine sediments have significantly longer half-lives (>900 yr) although half-life still varies substantially depending on environment (Table 3) (Flessa et al. 1993). The half-lives of *Chione* spp. in beach cheniers increase with distance from the shoreline, but the half-lives are within the estimate range for the adjacent tidal flat (Table 3) (Kowalewski et al. 1998; Flessa et al. 1993). This may be an indication of the importance of meteoric dissolution on shell loss in this environment. Estimates from the Gulf of California range from 18 to 1165 yr, but half-life estimates from ~300 to ~550 yr are the most common. Flessa (1998) dated *Cerastoderma edule* shells from intertidal, subtidal, and offshore siliciclastic sediments of the temperate North Sea. *Cerastoderma* is an intertidal bivalve, but both the intertidal and subtidal environments yielded half-lives of

TABLE 3. Estimates of shell half-lives from marine environments based on published studies. Only studies with direct dates of individuals shells are included. If a study used a particular size criterion it is indicated in the Taxon column (x refers to the maximum shell dimension, h refers to the shell height).

Taxon	Sediment	Environment	Water depth (m)	Location		Half-life (yr)							n	Reference	Notes
							Published data			Recalibrated ages					
				Lat.	Country	Reported	Best	Low	High	Best	Min	Max			
Chione spp.	Siliciclastic	Tidal Flat – surface	<0	31°N	Mexico		616	338	967	551	292	883	17	Flessa et al. 1993	
>28 mm (x)		Tidal Channel – surface	>0				337	220	511	268	150	447	13		
		Tidal Flat – core					1243	989	1570	1165	923	1475	8		
		Tidal Channel – core					981	719	1373	906	633	1274	9		
Chione spp.	Siliciclastic	Flat – surface	>0	31°N	Mexico					559	266	895	8	Martin et al. 1996	
Chione spp.	Siliciclastic	Fan-delta (E)	~2	27°N	Mexico	165				77	26	147	24	Meldahl et al. 1997	
>25 mm (x)		Fan-delta (W)	~2	27°N		165				91	34	160	24		
		Pocket bay	~2	27°N		90				18	7	48	24		
		Tidal channel	>0	31°N		285				See Flessa et al.			13		
		Tidal flat	<0	31°N		550				See Flessa et al.			17		
	Siliciclastic	Frisian Coast	~0		Germany					2733	1275	4051	9	Flessa 1998	
		Frisian Coast	10–12							2525	1272	3796	10		
		Off-shore	16–59							4856	3666	5968	16		
Chione fluctifraga		Chenier 1–62 cm	<0	31°N	Mexico		93	77	108				20	Kowalewski et al. 1998	
		Chenier 1–70 cm					126	107	149				20	Kowalewski et al. 2000	
		avg. Chenier 1					109	96	124				40		
		Chenier 2–70 cm					401	319	491				20		
		Chenier 3–20 cm					350	263	431				18		
		Chenier 3–70 cm					389	304	477				21		
		Chenier 3–130 cm					379	309	449				19		
		Chenier 3–150 cm					286	184	413				7		
		avg. Chenier 3					363	320	404				65		
		Chenier 4–20 cm					605	522	687				19		
		Chenier 4–40 cm					522	481	562				19		
		avg. Chenier 4					562	512	614				38		
Bouchardia rosea	Mixed	Shelf	6–23	23°S	Brazil		210							Carroll et al. 2003	Locations – distinct age-distributions
		Locality 1	6				117	74	157				19		
>1 mm (x)		Locality 2	23				218	174	264				20		(measurements made but not reported)
		Locality 3	16				404	239	619				21		
		Locality 4	9				530	246	866				22		
		avg.					326	234	439				79		

TABLE 3. Continued.

Taxon	Sediment	Environment	Water depth (m)	Location		Half-life (yr)							n	Reference	Notes
							Published data			Recalibrated ages					
				Lat.	Country	Reported	Best	Low	High	Best	Min	Max			
Pitar spp.,	Carbonate	Mud	3–44	9°N	Panama		118	61	188				12	Kidwell et al. 2005	
Macoma		Grassbed	1–5				406	26	1151				6		
spp.,		Reef hardground	1–30				471	15	1122				6		
Codakia	Siliciclastic	Mud	9–35				500	88	1075				8		
(*Ctena*)		Sand	9–10				1587	565	2935				7		
spp., *Callista eucymata*	Mixed	Peri-reefal (Mango)	4–10				208	88	359				6		
>>6 mm (h)		Peri-reefal (Bocas)	15		(Bocas)		657	223	1091				5		
Tellina casta	Carbonate	Lagoon – Small / Shallow	7.1	18°S	Australia		222	49	523				10	Kosnik et al. 2007	Small / Shallow
>4 mm		Lagoon – Small / Deep					323	211	453				30		Small / Deep
		Lagoon – Large / Shallow					44	41	47				9		Large / Shallow
		Lagoon – Large / Deep					717	540	885				34		Large / Deep
Ethalia	Carbonate	Lagoon – subsurface	7.1	18°S	Australia		925	765	1086				51	This paper	Deep
Natica							630	482	775				51		Deep
Tellina							574	443	708				125		Deep
Turbo							1229	1044	1442				38		Deep
Tellina	Carbonate	Lagoon – subsurface	6.7				131	102	164				120		Deep
Turbo							552	386	726				43		Deep

~2600 (1270–4050) yr (Table 3). *Cerastoderma* from offshore environments had half-lives >4800 yr. These half-lives are nearly an order of magnitude greater than the half-lives from the Gulf of California. Panamanian bivalve half-lives range from 118 to 1587 yr depending on environment, although the uncertainty on these estimates is high because of the small sample sizes involved (Table 3) (Kidwell et al. 2005). Brazilian brachiopod half-lives range from 117 to 530 yr depending on the sampling locality, but the half-lives do not appear to correlate with water depth or distance from shore (Table 3) (Carroll et al. 2003).

Although these estimates cover two orders of magnitude, from ~20 to ~2600 yr, most estimates are within a much narrower range from ~100 to ~1000 yr. The half-life estimates from Rib Reef fall squarely in this range (~70 to ~1300 yr). The present study suggests that morphological characteristics can account for a ten-fold difference in half-life for shells from the same environment. Shell size accounts for a twofold difference within *Tellina* shells, but small-scale spatial heterogeneity is implicated in the greater-than-threefold difference in *Tellina* half-life and the twofold difference in *Turbo* opercula half-life. These results fit within a consistent, albeit sparse, suite of previous studies. There is clearly room to examine the half-lives of additional taxa and environments.

Conclusions and Implications

1. Surface sediments of mid-shelf Great Barrier Reef lagoons are distinct from sediments deeper than ~20 cm. The sediments above 20 cm are finer grained than deeper sediments, with only few large (>4 mm) constituents, most of which are all living molluscs.
2. Molluscan remains indicate that the >4 mm sieve fraction below 20 cm is age homogeneous. In the short stratigraphic sequences recorded here (20 to 125 cm), intact shells from all four molluscan species are stratigraphically disordered: shell position is a poor indicator of relative shell age and hence sediment age.
3. Shell durability (here, size, density, thickness, and shape) are important predictors of shell half-life.
4. Shell ages and inferred half-lives vary on small spatial scales. Taphonomic variation at a small spatial scale (<100 m) can exceed within-core differences.
5. The extent of time-averaging constrains the degree to which these fossil assemblages can be used to address questions of paleoecology or microstratigraphic studies of evolution. Importantly, shell samples within at least 1 m of vertical separation record the same time interval because of thorough vertical mixing in this modern carbonate environment.

Acknowledgments

The author list is alphabetical following the lead author, and each coauthor contributed time, thought, and effort to this paper. We thank R. Gegg, G. Ewels, and M. LaBarbera for key contributions to the sampling equipment and methodology; the divers who assisted with sample collection (W. Beynon, N. Bigourdan, D. Feary, E. Graham, A. Kerswell, J. Livingstone, J. Maddams, W. Robbins, A. Swaddling, and E. Walker); the crew of the R/V *James Kirby* (D. Battersby, M. O'Leary, and G. Topping); the Tidal Unit of Maritime Safety Queensland for providing tidal measurements and advice on water depth corrections; J. Bright and C. Orem for generating the AAR data; S. Whittaker for assistance with SEM imagery; J. Wingerath for preparing shell cross-sections; B. Boykins for assistance with the acid dissolution experiment; T. Nickens for assistance in accessing the Invertebrate Zoology collections at the National Museum of Natural History; E. Harper, E. Hunt, S. Kidwell, R. Lockwood, W. Ponder, and K. Wilson for helpful advice during the creation of this manuscript; and K. Parsons-Hubbard, R. Krause, and S. Kidwell for helpful and thoughtful reviews of the manuscript. This research was funded by Australian Institute of Nuclear Science and Engineering awards 05/098 and 06/100 (^{14}C AMS analyses), Ian Potter Foundation (sample collection), PADI Foundation research

grant 248 (sample collection), James Cook University Merit Research Grant (development of sampling methodology), National Science Foundation grant EAR-0620455 (AAR analyses), and a Wilson grant (M.A.K. support).

Literature Cited

Best, M. M. R., T. C. W. Ku, S. M. Kidwell, and L. M. Walter. 2007. Carbonate preservation in shallow marine environments: unexpected role of tropical siliciclastics. Journal of Geology 115:437–456.

Bottjer, D. J., and W. I. Ausich. 1986. Phanerozoic development of tiering in soft substrata suspension-feeding communities. Paleobiology 12:400–420.

Bradshaw, C., and T. P. Scoffin. 2001. Differential preservation of gravel sized bioclasts in Apheid-versus Callianassid-bioturbated muddy reef sediments. Palaios 16:186–191.

Carroll, M., M. Kowalewski, M. G. Simões, and G. A. Goodfriend. 2003. Quantitative estimates of time-averaging in terebratulid brachiopod shell accumulations from a modern tropical shelf. Paleobiology 29:381–402.

Cooper, R. A., P. A. Maxwell, J. S. Crampton, A. G. Beu, C. M. Jones, and B. A. Marshall. 2006. Completeness of the fossil record: estimating losses due to body size. Geology 34:241–244.

Cummins, H., E. N. Powell, R. J. Stanton, and G. Staff. 1986. The rate of taphonomic loss in modern benthic habitats: how much of the potentially preservable community is preserved? Palaeogeography, Palaeoclimatology, Palaeoecology 52:291–320.

Cutler, A. H., and K. W. Flessa. 1990. Fossils out of sequence: computer simulations and strategies for dealing with stratigraphic disorder. Palaios 5:227–235.

Davies, D. J., E. N. Powell, and R. J. Stanton Jr. 1989. Relative rates of shell dissolution and net sediment accumulation: a commentary: can shell beds form by the gradual accumulation of biogenic debris on the sea floor? Lethaia 22:207–212.

Flessa, K. W. 1998.Well-traveled cockles: shell transport during the Holocene transgression of the southern North Sea. Geology 26:187–190.

Flessa, K. W., and T. J. Brown. 1993. Selective solution of macroinvertebrate calcareous hard parts: a laboratory study. Lethaia 16:193–205.

Flessa, K. W., A. H. Cutler, and K. H. Meldahl. 1993. Time and taphonomy: quantitative estimates of time-averaging and stratigraphic disorder in a shallow marine habitat. Paleobiology 19:266–286.

Glover, C. P., and S. M. Kidwell. 1993. Influence of organic matrix on the post-mortem destruction of molluscan shells. Journal of Geology 101:729–747.

Harper, E. M. 2000. Are calcitic layers an effective adaptation against shell dissolution in the Bivalvia? Journal of Zoology 251:179–186.

Hua, Q., G. E. Jacobsen, U. Zoppi, E. M. Lawson, A. A. Williams, and M. J. McGann. 2001. Progress in radiocarbon target preparation at the ANTARES AMS centre. Radiocarbon 43:275–282.

Hughen, K. A., M. G. L. Baillie, E. Bard, A. Bayliss, J. W. Beck, C. Bertrand, P. G. Blackwell, C. E. Buck, G. Burr, K. B. Cutler, P. E. Damon, R. L. Edwards, R. G. Fairbanks, M. Friedrich, T. P. Guilderson, B. Kromer, F. G. McCormac, S. Manning, C. Bronk Ramsey, P. J. Reimer, R. W. Reimer, S. Remmele, J. R. Southon, M. Stuiver, S. Talamo, F. W. Taylor, J. van der Plicht, and C. E. Weyhenmeyer. 2004. Marine04 marine radiocarbon age calibration, 0–26 Cal Kyr BP. Radiocarbon 46:1059–1086.

Kaufman, D. S., and W. F. Manley. 1998. A new procedure for determining DL amino acid ratios in fossils using reverse phase liquid chromatography. Quaternary Science Reviews 17:987–1000.

Kershaw, P. J., D. J. Swift, and D. C. Denoon. 1988. Evidence of recent sedimentation in the eastern Irish Sea. Marine Geology 85:1–14.

Kidwell, S. M. 2001. Preservation of species abundance in marine death assemblages. Science 294:1191–1194.

———. 2002. Mesh-size effects on the ecological fidelity of death assemblages: a meta-analysis of molluscan live-dead studies. Geobios 35:107–119.

———. 2005. Shell composition has no net impact on large-scale evolutionary patterns in mollusks. Science 307:914–917.

Kidwell, S. M., M. M. R. Best, and D. S. Kaufman. 2005. Taphonomic trade-offs in tropical marine death assemblages: differential time-averaging, shell loss, and probable bias in siliciclastic vs. carbonate facies. Geology 33:729–732.

Kosnik, M. A., and D. S. Kaufman. 2008. Identifying outliers and assessing the accuracy of amino acid racemization measurements for use in geochronology. II. Data screening. Quaternary Geochronology 3:328–341.

Kosnik, M. A., D. Jablonski, R. Lockwood, P. M. Novak-Gottshall. 2006. Quantifying molluscan body size in evolutionary and ecological studies: maximizing the return on data-collection efforts. Palaios 21:588–697.

Kosnik, M. A., Q. Hua, G. E. Jacobsen, D. S. Kaufman, R. A. Wüst. 2007. Sediment mixing and stratigraphic disorder revealed by the age-structure of *Tellina* shells in Great Barrier Reef sediment. Geology 35:811–814.

Kosnik, M. A., D. S. Kaufman, and Q. Hua. 2008. Identifying outliers and assessing the accuracy of amino acid racemization measurements for use in geochronology. I. Age calibration curves. Quaternary Geochronology 3:308–327.

Kowalewski, M. 1996. Time-averaging, overcompleteness, and the fossil record. Journal of Geology 104:317–326.

Kowalewski, M., G. A. Goodfriend, and K. W. Flessa. 1998. The high-resolution estimates of temporal mixing in shell beds: the evils and virtues of time-averaging. Paleobiology 24:287–304.

Kowalewski, M., G. E. A. Serrano, K. W. Flessa, and G. A. Goodfriend. 2000. Dead delta's former productivity: two trillion shells at the mouth of the Colorado River. Geology 28: 1059–1062.

Martin, R. E., J. F. Wehmiller, M. S. Harris, and W. D. Liddell. 1996. Comparative taphonomy of bivalves and foraminifera from Holocene tidal flat sediments, Bahía la Choya, Sonora, Mexico (Northern Gulf of California): taphonomic grades and temporal resolution. Paleobiology 22:80–90.

Meldahl, K. H. 1987. Sedimentologic and taphonomic implications of biogenic stratification. Palaios 2:350–358.

Meldahl, K. H., K. W. Flessa, and A. H. Cutler. 1997. Time-averaging and postmortem skeletal survival in benthic fossil assemblages: quantitative comparisons among Holocene environments. Paleobiology 23:207–229.

Olszewski, T. D. 2004. Modeling the influence of taphonomic destruction, reworking, and burial on time-averaging in fossil accumulations. Palaios 19:39–50.

Patterson, W. P., and L. M. Walter. 1994. Syndepositional diagenesis of modern platform carbonates: evidence from isotopic and minor element data. Geology 22:127–130.

Perry, C. T. 1998. Grain susceptibility to the effects of microboring: implications for the preservation of skeletal carbonates. Sedimentology 45:39–51.

R Development Core Team. 2008. R: a language and environment for statistical computing. R Foundation for Statistical Computing, Vienna. http://www.R-project.org.

Sanders, D. 2003. Syndepositional dissolution of calcium carbonate in neritic carbonate environments: a geological recognition,

processes, potential significance. Journal of African Earth Sciences 36:99–134.

Stuiver M., P. J. Reimer, E. Bard, J. W. Beck, G. S. Burr, K. A. Hughen, B. Kromer, G. McCormac, J. van der Plicht, and M. Spurk. 1998. INTCAL 98 radiocarbon age calibration, 24,000–0 cal BP. Radiocarbon 40:1041–1083.

Tudhope, A. W. 1989. Shallowing upwards sedimentation in a coral reef lagoon, Great Barrier Reef of Australia. Journal of Sedimentary Petrology 59:1036–1051.

Tudhope, A. W., and M. J. Risk. 1985. The rate of dissolution of carbonate sediments by microboring organisms, Davies reef, Australia. Journal of Sedimentary Petrology 55:400–447.

Tudhope, A. W., and T. P. Scoffin. 1984. The effects of *Callianassa* bioturbation on the preservation of carbonate grains in Davies reef lagoon, Great Barrier Reef, Australia. Journal of Sedimentary Petrology 54:1091–1096.

Walbran, P. D. 1996. ^{210}Pb and ^{14}C as indicators of Callianassid bioturbation in coral reef sediment. Journal of Sedimentary Research 66:259–264.

Walbran, P. D., R. A. Henderson, J. W. Faithful, H. A. Polach, R. J. Sparks, G. Wallace, and D. C. Lowe. 1989. Crown-of-thorn starfish outbreaks on the Great Barrier Reef: a geological perspective based on the sediment record. Coral Reefs 8:67–78.

Walter, L. M., and E. A. Burton. 1990. Dissolution of recent platform carbonate sediments in marine pore fluids. American Journal of Science 290:601–643.

Wright, P., L. Cherns, and P. Hodges. 2003. Missing molluscs: field testing taphonomic loss in the Mesozoic through early large-scale aragonite dissolution. Geology 31:211–214.

Zuschin, M., and R. J. Stanton Jr. 2001. Experimental measures of shell strength and its taphonomic implications. Palaios 16:161–170.